JOURNAL OF VIROLOGY, Sept. 2006, p. 9039–9052 Vol. 80, No. 18
0022-538X/06/$08.00+0 doi:10.1128/JVI.01013-06

Proteomic and Biochemical Analysis of Purified Human Immunodeficiency Virus Type 1 Produced from Infected Monocyte-Derived Macrophages

Elena Chertova,[1]* Oleg Chertov,[2] Lori V. Coren,[1] James D. Roser,[1] Charles M. Trubey,[1] Julian W. Bess, Jr.,[1] Raymond C. Sowder II,[1] Eugene Barsov,[1] Brian L. Hood,[2] Robert J. Fisher,[2] Kunio Nagashima,[2] Thomas P. Conrads,[2] Timothy D. Veenstra,[2] Jeffrey D. Lifson,[1] and David E. Ott[1]

AIDS Vaccine Program, Basic Research Program,[1] and Research Technology Program,[2] SAIC—Frederick, Inc., NCI—Frederick, Frederick, Maryland 21702

Received 17 May 2006/Accepted 24 June 2006

Human immunodeficiency virus type 1 (HIV-1) infects CD4$^+$ T lymphocytes and monocytes/macrophages, incorporating host proteins in the process of assembly and budding. Analysis of the host cell proteins incorporated into virions can provide insights into viral biology. We characterized proteins in highly purified HIV-1 virions produced from human monocyte-derived macrophages (MDM), within which virus buds predominantly into intracytoplasmic vesicles, in contrast to the plasmalemmal budding of HIV-1 typically seen with infected T cells. Liquid chromatography-linked tandem mass spectrometry of highly purified virions identified many cellular proteins, including 33 previously described proteins in HIV-1 preparations from other cell types. Proteins involved in many different cellular structures and functions were present, including those from the cytoskeleton, adhesion, signaling, intracellular trafficking, chaperone, metabolic, ubiquitin/proteasomal, and immune response systems. We also identified annexins, annexin-binding proteins, Rab proteins, and other proteins involved in membrane organization, vesicular trafficking, and late endosomal function, as well as apolipoprotein E, which participates in cholesterol transport, immunoregulation, and modulation of cell growth and differentiation. Several tetraspanins, markers of the late endosomal compartment, were also identified. MDM-derived HIV contained 26 of 37 proteins previously found in exosomes, consistent with the idea that HIV uses the late endosome/multivesicular body pathway during virion budding from macrophages.

As an RNA virus with limited coding capacity, human immunodeficiency virus type 1 (HIV-1) subverts cellular pathways and processes to facilitate many aspects of its replication cycle. It is known that a variety of cellular factors are involved in HIV-1 assembly and budding (13, 20, 42, 44). Typically, HIV-1 is observed by electron microscopy to assemble at and bud from the plasma membrane in T cells and the epithelial cell lines that serve as models for HIV-1 assembly studies (23). In contrast, in macrophages, one of the primary target cell populations in vivo, HIV-1 appears to assemble mostly at internal late endosomal and multivesicular body (MVB) membranes and then bud into these vesicular structures, observable in electron micrographs as internal virion-filled compartments (48, 54, 55, 59). After budding into MVB, these virion-laden vesicles are presumably transported to the cell surface and virus is released from the cell by a normal exocytotic fusion of these structures with the plasma membrane, thereby releasing the contents of the MVB (54, 55).

To date, the differences in viral and cellular protein interactions involved in assembly and budding at the plasma membrane versus the late endosomal assembly pathway remain unclear. Clues to the location and the mechanism by which HIV-1 buds can be provided by the cellular proteins that are incorporated into virions. In the case of macrophage-derived virus, the presence of HLA class II and other late endosomal proteins supports the assembly and budding of HIV-1 in the late-endosome/MVB compartment (45). Also, cellular proteins have been used to identify the cell type that produced the HIV-1 found in patient plasma (37).

In addition to being potential fingerprints for the assembly pathway, cellular proteins found in virions may also play roles in viral pathobiology. The incorporation of cellular proteins such as HLA class II, ICAM-1, and tetraspanins can affect the ability of HIV-1 to infect host cells (7, 43). The presence of HLA class II on virions may contribute to immunopathogenesis, as noninfectious virions carrying HLA class II can induce apoptosis in primary T cells in vitro (18).

Several groups have studied the cellular proteins incorporated into HIV-1 virions produced from lymphocytes and in epithelial cell model systems (reviewed in references 7, 49, and 71); however, the cellular protein content of virions produced from macrophages remains largely unstudied (37, 45). This cell type not only appears to use alternate assembly and budding pathways but also is an important cell lineage for HIV-1 transmission, establishment and maintenance of infection, and pathogenesis (36, 37, 57).

The analysis of cellular proteins in virions is complicated by the presence of non-virion protein-containing particles that can contaminate even virion preparations extensively purified by density gradient centrifugation (1, 25). These particles, mostly microvesicles and exosomes, are produced as part of normal cellular physiology and have been implicated in cell-to-cell signaling and immune activation/surveillance (15, 31, 32, 55, 69). A key difference between the two types of particles is that microvesicles are defined as those particles that bud

* Corresponding author. Mailing address: AIDS Vaccine Research Program, SAIC—Frederick, Inc., NCI—Frederick, Frederick, MD 21702. Phone: (301) 846-1455. Fax: (301) 846-5588. E-mail: chertova@ncifcrf.gov.

from the plasma membrane, while exosomes form by budding into late endosomes/MVB vesicles that ultimately fuse with the plasma membrane, releasing these particles from the cell (69). Despite this difference, the two particle types share similarities in morphology and other properties. While these vesicles can be quite heterogeneous, a certain population of these particles has the same density as and approximate size of virion particles, making them quite difficult to remove from virion preparations (1, 25). We have developed a technique by which these contaminating particles can be removed from virion samples by using CD45 affinity depletion with antibody-linked paramagnetic microbeads (72). This method exploits the fact that CD45 is present on many of these vesicles (19, 76) yet is excluded from HIV-1 particles (19, 45). Therefore, CD45 immunoaffinity depletion, combined with density centrifugation, produces highly purified virus preparations.

To better understand the assembly process in macrophages and to identify cellular proteins that might play a role in HIV-1 biology, we examined HIV-1 preparations produced from monocyte-derived macrophages (MDM) that were highly purified by density centrifugation and CD45 immunoaffinity depletion by using liquid chromatography (LC) coupled with electrospray ionization tandem mass spectrometry (MS/MS). Our analysis revealed a large number of cellular proteins not previously described for HIV-1, in addition to proteins previously identified from non-macrophage-derived virus. These results provide important leads for the continued study of HIV-1 assembly, infection, and pathogenesis.

MATERIALS AND METHODS

Virus preparations. Infectious CCR5-tropic HIV-1 stocks were produced by transfecting 293T cells with the full-length infectious molecular clone NLAD8 (21) by using TransIt 293 reagent (Mirus Corp., Madison, WI). Elutriated monocytes were obtained from HIV-negative donors through the NIH Department of Transfusion Medicine under an NIH institutional research board-approved protocol. To generate macrophages, monocytes (approximately 10^8 cells) were cultured for seven days on hydrogel-treated plates (ultralow-attachment six-well clusters [catalog no. 3471; Corning, Acton, MA) in RPMI 1640, supplemented with 10% (vol/vol) fetal bovine serum, 2 mM L-glutamine, 100 U per ml penicillin, and 100 μg per ml streptomycin. All cell culture products were obtained from Invitrogen (Carlsbad, CA). One half of the MDM from each donor were infected with virus, while the other half served as an uninfected control. Infections were carried out at a multiplicity of infection of >4, and virus production was monitored by a reverse transcriptase assay (28). Input virus was removed from infected cultures by two washings with medium before MDM-derived virus was collected. Culture supernatants were collected over a series of weeks and frozen. Supernatants from the cultures were then thawed, pooled, and clarified by centrifugation (10 min at 2,000 × *g*) prior to CD45 depletion (see below). All other virus preparations were produced from chronically infected cell lines and purified by sucrose density gradient centrifugation, as previously described (2). Viruses are designated according to the viral strain and cell line in which they were propagated, for example, SIV_{mne}/HuT-78 cl.E11S and $HIV\text{-}1_{MN}$/H9 clone 4.

CD45 immunodepletion. Virion and vesicle preparations were depleted with anti-CD45 paramagnetic microbeads (catalog no. 130-045-801; Miltenyi Biotec Inc., Southbridge, MA) as previously described (72) with the following modifications. Before use, the microbeads were captured from the stock suspension by applying a magnetic field using one of two Dynal (Brown Deer, WI) magnetic separators, MPC-S or MPC-L. Beads were then washed twice in phosphate-buffered saline (Invitrogen) and resuspended in their original volume. For depletion, clarified cell culture supernatants were treated with anti-CD45 microbeads at a concentration of 2 μl of beads per ml of supernatant, followed by a brief mixing. After 1 h at room temperature, the supernatants were placed in magnetic separators and incubated at 4°C for at least 20 h. CD45 immunoaffinity-depleted supernatants were then removed from the beads by pipetting and centrifuged at 120,000 × *g* at 4°C for 1 h to pellet virions. Beads were recovered and retained for immunoblot analysis. Fifty milliliters of combined cell culture supernatants from both uninfected and NLAD8-infected MDM cultures was CD45 depleted and density centrifuged to produce the uninfected control and virion preparations analyzed by mass spectrometry.

Immunoblot analysis. Immunoblot analyses were carried out as previously described (50). The sera used were rabbit anti-Env (reacting with both gp120 and gp41) (Fitzgerald, Concord, MA) and goat anti-$p24^{CA}$ (goat no. 81; AIDS Vaccine Program, NCI—Frederick). Monoclonal antibodies specific for p24 (AIDS Vaccine Program), CD45 (BD-Transduction Laboratories, Inc., San Diego, CA), CD63 (Santa Cruz Biotechnology, Inc., Santa Cruz, CA), and Tsg101 (Genetex, San Antonio, TX) were also used.

Fractionation and trypsin digestion of protein samples. Fifteen microliters of sample was prepared in Tris-glycine-sodium dodecyl sulfate (SDS) sample buffer containing 80 mM dithiothreitol (CalBiochem, La Jolla, CA) and incubated for 20 min at 56°C. After cooling at room temperature, the samples were alkylated at a final concentration of 400 mM of iodoacetamide and incubated for 30 min at room temperature in the dark. After alkylation, samples were separated by SDS-polyacrylamide gel electrophoresis (PAGE) on a 1.5-mm-thick 4 to 20% Tris-glycine gel (Invitrogen, Carlsbad, CA), followed by staining with 0.1% (wt/vol) Coomassie blue R-250 in a 40% (vol/vol) methanol, 5% (vol/vol) acetic acid, and water solution. The HIV-1-containing lane was sectioned into 17 contiguous pieces, which were subjected to proteolysis with bovine trypsin (Roche Diagnostics, Mannheim, Germany), according to a previously described protocol (8). The peptides extracted from the gel after digestion were purified by a method adopted from a previously described procedure (60), using 10-μl pipette tips fitted with C_{18} Empore Discs (3M, Minneapolis, MN) as a microcolumn.

MALDI-TOF mass spectrometry of tryptic digests. Aliquots containing one third of the extracted peptides were dissolved in 10 μl of 0.1% trifluoroacetic acid (TFA) and purified as described above. The purified material was eluted into a 0.65-ml Eppendorf tube with 2 μl of acetonitrile–0.1% TFA (50/50 [vol/vol]). A 0.5-μl aliquot of the sample was spotted onto a matrix-assisted laser desorption ionization (MALDI) target, followed by the addition of 0.5 μl of matrix solution (2 mg/ml alpha-cyano-4-hydroxycinnamic acid in acetonitrile–0.1% TFA [50/50 {vol/vol}]), containing 10 mM ammonium dihydrogen phosphate, as suggested in reference 79. The mixture was allowed to air dry before analysis. A Voyager-DE Pro time of flight (TOF) mass spectrometer (Perseptive, Houston, TX) was used for analysis. The accelerating voltage was 20 kV, guide wire 0.05%, and grid voltage 95%. The instrument was operated in linear mode under positive ion conditions. A nitrogen laser was used at 337 nm with 150 laser shots averaged per spectrum. Calibration was performed using instrument default settings, and data analysis was carried out using the Data Explorer software included with the Voyager mass spectrometer.

RPLC-MS/MS of tryptic digests and database search. The remaining two thirds of the peptide samples was dried using vacuum centrifugation and resuspended in 6 μl of 0.1% (vol/vol) TFA. The sample was then analyzed by microcapillary reversed-phase liquid chromatography (μRPLC) using an Agilent 1100 capillary LC system (Agilent Technologies, Inc., Palo Alto, CA), coupled online to an ion trap mass spectrometer (LTQ; Thermo Electron, San Jose, CA). Reversed-phase separations were performed using 75-μm-inside-diameter, 360-μm-outside-diameter, 10-cm-long capillary columns (Polymicro Technologies Inc., Phoenix, AZ) that were packed with 5 μm Jupiter C_{18} stationary phase slurry (Phenomenex Inc., Torrence, CA). After sample injection, a 20-min wash with 95% mobile phase A (0.1% [vol/vol] formic acid in water) was applied and peptides were eluted using a linear gradient of 5% mobile phase B (0.1% [vol/vol] formic acid in acetonitrile) to 45% mobile phase B over 40 min with a constant flow rate of 0.5 μl/min. The mass spectrometer was operated in a data-dependent MS/MS mode using a normalized collision-induced dissociation (CID) energy of 38%. Dynamic exclusion was applied to minimize redundant selection of peptides previously selected for CID. The temperature of the heated capillary was 180°C, and the electrospray voltage was 1.5 kV. Using SEQUEST (ThermoElectron, San Jose, CA), the CID spectra were compared against those of the EMBL nonredundant protein database. Only peptides having cross-correlation (X_{corr}) cutoffs of 1.9 for $[M + H]^{1+}$, 2.2 for $[M + 2H]^{2+}$, and 3.5 for $[M + 3H]^{3+}$ and with delta cross-correlation scores (ΔCn) of at least 0.09 (65) were considered legitimate identifications. These SEQUEST criteria thresholds have been determined previously to result in a 95% confidence level in peptide identification (77).

Transmission electron microscopy. Micrographs of positive-stained virions were obtained as previously described (27).

RP-HPLC separation and analysis of viral proteins. Virus sample was disrupted in 8 M guanidine-HCl (Pierce, Rockford, IL) and fractionated by high-performance liquid chromatography (HPLC) to isolate viral proteins under nonreducing conditions. HPLC was performed at a flow rate of 300 μl/min on 2.1- by

100-mm Poros R2/H narrow bore column (Boehringer Mannheim GmbH, Germany), using aqueous acetonitrile-trifluoroacetic acid solvents and a Shimadzu HPLC system equipped with LC-10AD pumps, a SCL-10A system controller, a CTO-10AC oven, a FRC-10A fraction collector, and a SPD-M10AV diode array detector. The gradient of buffer B (0.1% trifluoracetic acid in acetonitrile) was as follows: 10% to 36.5%, 12 min; 36.5% to 37%, 4 min; 37% to 41%, 7 min; 41% to 70%, 12 min; and 70%, 5 min. A temperature of 55°C was maintained during HPLC separation. Peaks were detected by UV absorption at 206 and 280 nm and analyzed by SDS-polyacrylamide gel electrophoresis. Quantitation of purified proteins was performed by dual-color fluorescent protein gel analysis.

Dual-color fluorescent protein gel analysis. Proteins from lysed virus preparations and HPLC fractions were resolved by SDS-PAGE on 4 to 20% Tris-glycine gels (Invitrogen) under reducing conditions. The $p24^{CA}$ and $gp120^{SU}$ content of the samples were determined by a two-color fluorescence staining assay. Gels with virus samples and a dilution series of purified protein standards were stained with two fluorescent dyes (Molecular Probes, Eugene, OR), SYPRO Pro-Q Emerald (green fluorescence) to detect glycoproteins, such as Env (envelope glycoprotein complex), and SYPRO Ruby (red fluorescence) to detect all proteins, including $p24^{CA}$. Stained gels were analyzed for fluorescence at 520 nm with UV excitation by using a VersaDoc 3000 imaging system (Bio-Rad Laboratories, Hercules, CA). The $gp120^{SU}$ and $p24^{CA}$ contents of each virion sample were calculated by using the Quantity One software package (Bio-Rad Laboratories) by interpolating the integrated pixel density signals from the unknown samples onto a standard curve derived from a linear regression of density values for serial dilutions of highly purified, quantitative amino acid analysis quantified standards, either recombinant vaccinia-produced $HIV\text{-}1_{MN}$ $gp120^{SU}$ (generously provided by B. Puffer and R. Doms, University of Pennsylvania, Philadelphia, PA) or $HIV\text{-}1_{MN}$ virion-derived $p24^{CA}$ (AIDS Vaccine Program, Basic Science Program, NCI—Frederick, Frederick, MD). Well characterized reference preparations of SIV_{mne}/HuT-78 cl.E11S and $HIV\text{-}1_{MN}$/H9 clone 4 (AIDS Vaccine Program, Basic Science Program, NCI—Frederick, Frederick, MD) were used to validate this procedure (10).

RESULTS

To examine the proteins found in virions produced by monocyte-derived macrophages, we produced two human MDM cultures from the same donor. One was infected with a CCR5-tropic HIV_{NLAD8} stock, while the other served as an uninfected control. Thin-section transmission electron microscopy of infected cells revealed that most of the HIV-1 observed was found inside the cell in internal vesicular structures (data not shown), consistent with previous findings that HIV-1 assembles and buds into internal structures in macrophages (48) that have been identified as late endosomes and MVBs (54).

To remove cellular vesicles from virions in cell culture supernatants, we CD45 immunoaffinity depleted clarified cell culture supernatants from these parallel cultures of uninfected and HIV_{NLAD8}-infected MDM by using CD45-antibody-coupled paramagnetic microbeads. This depletion method can remove more than 98% of the CD45 protein from T-cell-derived virus preparations (72). After depletion, the treated supernatants were subjected to our standard density centrifugation procedure to pellet virions away from soluble proteins and other cellular debris. The CD45-depleted preparations as well as the CD45-selected bead-bound fractions (all samples were 5% of the total material by volume) from the uninfected and HIV-infected MDM cultures were analyzed by immunoblot and SDS-PAGE analyses (Fig. 1). CD45 and $p24^{CA}$ immunoblot analyses (Fig. 1A) showed that while there was no detectable CD45 signal in the supernatant samples (the CD45-depleted fraction), there was an evident CD45 signal in the bead sample (the CD45-containing fraction), indicating that most of the CD45 was removed from both infected and uninfected materials. In addition to the CD45 signal in the bead sample, there is a 28-kDa band corresponding to the immunoglobulin light chain (Fig. 1A). This is likely mouse immunoglobulin light chain released from the heavy chain-microbead complex in reduced SDS-PAGE samples and detected by the anti-mouse secondary antibody employed in the analysis. Reacting the same blot with $p24^{CA}$ antiserum showed that virus was present in the CD45-depleted virus sample and not in the CD45-selected bead-bound sample (Fig. 1A).

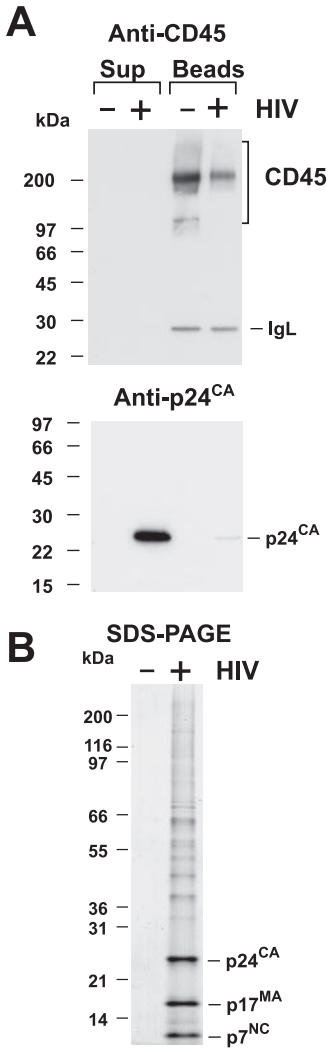

FIG. 1. Analysis of CD45-depleted HIV. (A) Immunoblots of CD45-depleted virion preparations (equal amounts by volume) isolated from parallel uninfected (−) and infected (+) cell cultures are presented. Samples from the immunoaffinity-depleted supernatant (Sup) and anti-CD45 bead fractions are identified above their respective lanes. Antibody or antiserum used is indicated above each blot. IgL, immunoglobulin light chain. (B) An analytical Coomassie blue-stained SDS-PAGE gel of CD45-depleted uninfected (−) and HIV-infected (+) preparations (equal amounts by volume) produced from MDM is shown.

The removal of contaminating vesicles from a virus sample should also be reflected in the removal of cellular proteins. An analytical-scale SDS-gel electrophoresis analysis of the CD45-immunodepleted and density-purified samples (3% of the total material by volume) prepared from infected and noninfected cells revealed that all of the detectable protein was removed

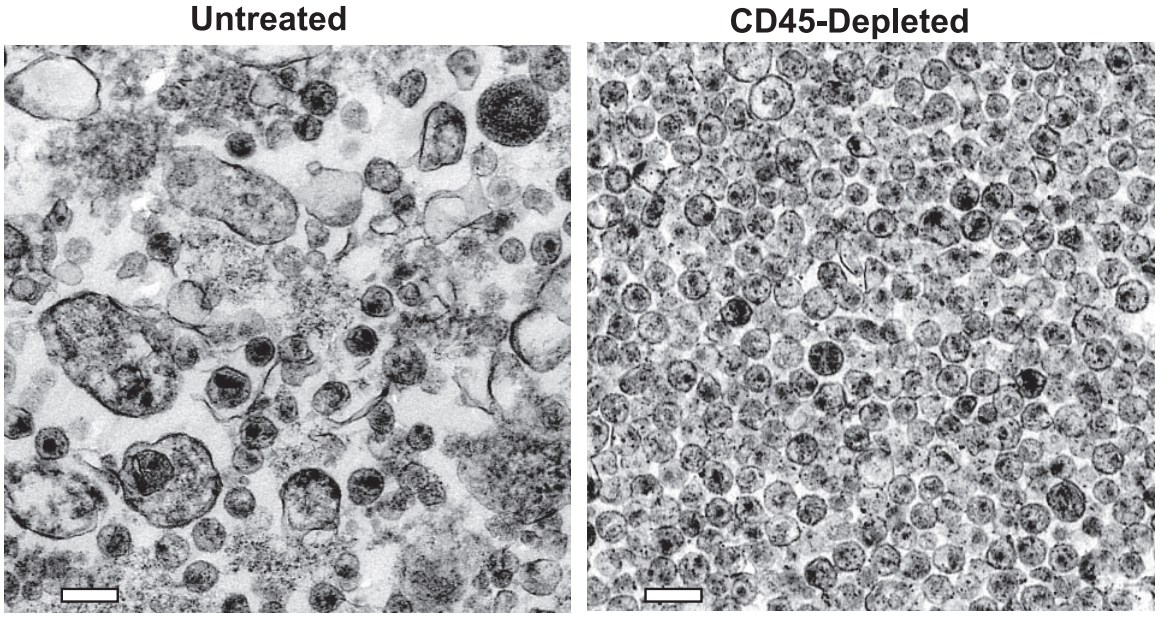

FIG. 2. Electron microscopy of HIV-1. Thin-section transmission electron micrographs of untreated and CD45-depleted virus preparations are shown. Samples are identified above their respective micrographs. A white 200-nm bar has been added to each micrograph for reference.

from the noninfected MDM samples, while viral proteins, as well as cellular proteins, still remained in the infected MDM preparations (Fig. 1B). Thus, the CD45 depletion and density centrifugation removed all of the detectable protein from the uninfected preparation.

Electron microscopy of virion preparations. To directly examine the removal of nonviral particles, we analyzed samples of the HIV-1 produced from MDM, processed with and without CD45 depletion, by transmission electron microscopy (Fig. 2). The untreated HIV-1 preparation contained a relatively small number of virions and an abundance of nonviral particles. In contrast, the CD45-depleted virion preparation contained mostly virions and few if any nonviral particles. These data are consistent with our previous observations (72), as well as with the biochemical data obtained for the same specimens, and directly demonstrate that CD45 depletion effectively removed vesicular contamination from the MDM-derived virion preparations.

Proteomics of CD45-depleted MDM-derived HIV. To identify proteins in HIV-1 produced from macrophages, the CD45-depleted HIV-1 preparation (corresponding to 2 μg of HIV-1 $p24^{CA}$, 30% of the total volume) was fractionated using a preparative-scale SDS-PAGE gel separation. Before SDS-PAGE, the cysteinyl residues within the samples were reduced and alkylated to avoid spontaneous intermolecular disulfide bond formation during electrophoresis. The CD45-depleted virion sample contained a large number of bands with a wide range of sizes (Fig. 3). In contrast, an equal volume (also 30%) of the uninfected control sample, i.e., the CD45-depleted preparation from the uninfected macrophages produced and processed in parallel, contained no detectable proteins in the preparative-scale Coomassie blue-stained gel (data not shown; results were identical to those in Fig. 1B). To analyze the proteins in the HIV-1 containing gel, the lane was sectioned into 17 contiguous slices (Fig. 3); each of these fractions was digested individually with trypsin, and the peptides generated were eluted from the gel by extraction. The LC-MS/MS technique requires a complete tryptic digest of the peptides with low levels of nonspecific cleavage that can occur with overdigestion of the sample with protease. To assess the quality of the eluted peptides, one-third of the peptide material extracted

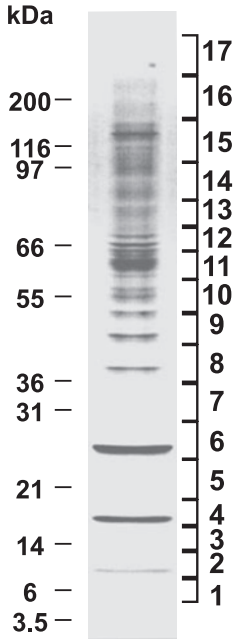

FIG. 3. Fractionated preparative SDS-PAGE gel. The Coomassie blue-stained preparative SDS-PAGE (4 to 20%) gel of the CD45-depleted virus sample is shown. Gel fractions taken are indicated at the right and the positions of molecular mass markers are denoted at the left.

TABLE 1. Cellular proteins in MDM-derived HIV-1[a]

Fraction (size range in kDa)	Protein name[b]	Mol mass (Da)[c]	Particle[d]	Location[e]	Function/structure in which protein is involved[f]	Accession no.[g]	No. of peptides
1 (5–7)	3′,5′-Cyclic phosphodiesterase B	124,376		M	Metabolism	Q13370	2
	Alpha-actinin 4 (F-actin cross linking protein)	104,854		C	Actin cytoskeleton	O43707	2
2 (8–11)	**S100A10 (p11)**	11,072		C, M	LE trafficking	P60903	5
	S100A11 (S100C)	11,740		C, M	Signaling	P31949	4
	S100A6	10,180		C, M	Signaling	P06703	2
	S100A8	10,835		C, M	Signaling	P05109	2
	Histone H4	11,236	Exo	N	Chromatin	P62805	3
	Beta-2-microglobulin	13,714	Vir	M	Antigen presentation	P61769	2
	Syndecan-2 (C-terminal fraction)	22,174 (P)		M	Adhesion	P34741	2
	Hypothetical protein (fractions 3 [2] and 15 [4])	15,258		?	?	Q3MIF5	2
3 (11–16)	**Epidermal fatty acid-binding protein (E-FABP)**	15,033		C	Lipid organization	Q01469	4
	Histone H2B	13,775	Exo	N	Chromatin	P62807	4
	Histone H3.1	15,273	Exo	N	Chromatin	P68431	2
	Profilin-1	14,923	Exo	C	Actin cytoskeleton	P07737	3
	Vesicle-associated membrane protein 8 (VAMP-8)	11,438		C	LE trafficking	Q9BV40	3
	Vacuolar ATP synthase subunit G1	13,626		C	Vesicular acidification	O75348	3
	Lysozyme C	16,537		S	Bacteriolysis	P61626	3
	Ubiquitin (fractions 4 [3], 6 [2], 8 [2], 10 [2], 12 [2], 15 [2])	8,565	Vir	C, N	UPS/protein trafficking	Q9UEF2	3
	Retinoic acid-binding protein II (CRABP-II)	15,562		C	Signaling	P29373	2
	Galectin-1	14,584		C, M, S	Signaling	P09382	2
	Coactosin-like protein	15,814		C	Actin cytoskeleton	Q14019	2
	Signal recognition particle 14-kDa protein (SRP14)	14,544		C	Secretion	P37108	2
	Syndecan-2 (mature protein)	22,174 (P)		M	Adhesion	P34741	2
4 (16–20)	**Cyclophilin A (fraction 5 [2])**	17,881	Vir	C	Protein folding	P62937	8
	GAPR-1	17,087		M	Membrane (Golgi, ER)	Q9H4G4	5
	Cofilin (fraction 5 [2])	18,502	Exo, Vir	C	Actin cytoskeleton	P23528	4
	Methylmalonyl-coenzyme A epimerase	18,749		?	?	Q96PE7	2
	RAD21-like 1	22,840		?	?	Q5W0X5	2
	Rho-related GTP-binding protein RhoG	21,309		M	Signaling	P84095	2
	40S ribosomal protein S16	16,314		C	Translation	P62249	2
	Ankyrin repeat domain 22	21,849		?	?	Q5VYY1	2
	Beta-glucan receptor isoform E	19,218		M	Innate immunity	Q96PA7	2
	Clathrin light chain A	27,077		M	Endocytosis	P09496	3
	Clathrin light chain B (fraction 3 [3])	25,190		M	Endocytosis	P09497	2
	COP9 signalosome complex subunit 7b	29,622		C	Signaling/neddylation	Q9H9Q2	2
	Forkhead box protein G1B	51,340		N	Transcription	P55315	2
	Galectin-9	39,518		S	Signaling	O00182	2
	HSPC069 isoform b	135,937		?	?	Q5QGN2	2
	Prolyl endopeptidase	80,749		C	Cellular protease	P48147	2
5 (20–24 kDa)	**Actin-related protein 2/3 complex subunit 4**	19,536		C	Actin cytoskeleton	P59998	5
	Vacuolar protein sorting (Vps) 29 human homolog	20,506		C, M	Vesicular trafficking	Q9UBQ0	2
	ARF-1 (ADP-ribosylation factor 1) (fraction 4 [3])	20,566		M	Vesicular trafficking	P84077	3
	Rap-1A (Ras-related protein)	20,987		M	Signaling	P62834	2
	CDC42	21,311		M	Actin cytoskeleton	P60953	2
	Cyclophilin B	22,742		ER	ER protein folding	P23284	2
	Tmp21	24,976		G	Golgi vesicle sorting	P49755	2
	Synaptogyrin-1	25,570		?	?	O43759	2
	CD81 (fraction 2 [2])	25,809	Exo, Vir	M	Signaling	P60033	1
	Desmoyokin (AHNAK) (fraction 2 [2])	312,493		C, N	Actin cytoskeleton	Q09666	2
	Desmoplakin (DP) (fraction 3 [3])	8,331,776		C	Actin cytoskeleton	P15924	3
	Junction plakoglobin (desmoplakin-3)	81,498		C, M	Actin cytoskeleton	P14923	3
	Tsg101	43,944	Exo, Vir	C	Vesicle sorting	Q99816	2
6 (24–29)	**CD9 (fractions 5 [3], 7 [4], 8 [5], 9 [2], 10 [2], 12 [2], 13 [2], and 14 [3])**	25,285	Exo	M	Signaling	P21926	7
	Syntenin 1	32,444	Exo	M	Actin cytoskeleton	O00560	6
	Peroxiredoxin 6	24,904		C	Redox control	P30041	6
	Triosephosphate isomerase (TPI)	26,538		C	Metabolism	P60174	6
	Rab7 (fraction 5 [4])	23,490	Exo	C	LE trafficking	P51149	5
	Phosphoglycerate mutase 1	28,673		C	Catabolism	P18669	4
	Rab8A	23,668		M	Vesicular trafficking	P61006	4
	Rab11	24,393	Exo	M	Vesicle trafficking	P62491	3
	Rab5C	23,483		M	Vesicular transport	P51148	3
	Rab35	23,025		M	Vesicle trafficking	Q15286	2
	Protein kinase C inhibitor protein 1 zeta/delta	27,745		C	Signaling	P63104	3
	B-cell receptor-associated protein 31	27,860		ER, G	ER-to-Golgi trafficking	P51572	3
	Glutathione *S*-transferase P	23,225		C	Redox control	P09211	3
	GTP-binding nuclear protein Ran	24,423		N, C	Nuclear shuttling	P62826	3
	LGALS3 protein variant (fraction 4 [3])	27,118		?	Lectin binding	Q59FR8	3
	Metalloproteinase inhibitor 2 (TIMP-2)	24,399		S	Protease inhibitor	P16035	2
	Protein kinase C inhibitor protein 1 beta/alpha	27,951		C	Signaling	P31946	2
	Hypothetical protein FLJ43237	24,474		?	?	Q6ZUX7	2
	Tetraspanin-14	30,691		?	?	Q8NG11	2
	CD258	26,351		C, M, S	Signaling	O43557	2

Continued on following page

TABLE 1—*Continued*

Fraction (size range in kDa)	Protein name[b]	Mol mass (Da)[c]	Particle[d]	Location[e]	Function/structure in which protein is involved[f]	Accession no.[g]	No. of peptides
	Vps28 (human homolog)	26,558		C	ESCRT I component	Q9UK41	2
	Rab1A	22,547		G	Golgi vesicular sorting	P62820	5
	Transforming protein RhoA	21,768		M	Signaling	P61586	4
	Peroxiredoxin 1	22,110		C	Redox control	Q06830	3
	Rac3	21,379		C, M	Signaling	P60763	2
	Renin receptor	39,008		M	Signaling	O75787	3
	SNARE protein Ykt6	22,418		ER, G	ER-to-Golgi transport	O15498	3
	Inositol oxygenase (fraction 4 [4])	33,010		C	Catabolism	Q9UGB7	2
	Rac1	21,450		M	Signaling	P63000	3
	Rac2	21,429		C	Signaling	P15153	2
	Rab10	22,541		M	Vesicular transport	P61026	2
	Rab13	22,774		C	Vesicular transport	P51153	2
	Rab5A	23,659		M	Endocytosis	P20339	2
	Rab8B	23,584		M	Vesicular transport	Q92930	2
	Ral-B	23,409		M	Signaling	P11234	2
	Rap-1b	20,825		M, C	Signaling	P61224	2
7 (29–34)	**Annexin A5**	35,805	Exo	M	Blood clotting	P08758	4
	PA28a proteasome subunit	28,723		C, N	UPS	Q06323	2
	eEF1A (HIV-1 protease fragment[h])	~30,000	Vir	C	Translation	Q05639	3
	HLA class II-DR	29,966	Exo	M	Antigen presentation	P01903	3
	Chloride intracellular channel protein 1 (NCC27)	26,792		N, M, C	Ion transport	O00299	2
8 (34–43)	**Annexin A2 (calpactin I heavy chain) (fractions 7 [3] and 9 [9])**	38,472	Exo	M	Exocytosis	P07355	27
	ApoE (fractions 2 [3], 3 [2], 4 [6], 5 [5], 6 [11], 7 [7], 9 [8], 10 [2], 12 [5], 13 [2], 14 [4], 15 [3], and 16 [2])	36,154		S	Cholesterol transport	P02649	25
	Annexin A1	38,583	Exo		Exocytosis	P04083	7
	CD53 (fractions 4 [1], 5 [1], 6 [1], and 10 [1])	24,341 (G)	Exo	M	Signaling	P19397	2
	Glyceraldehyde-3-phosphate dehydrogenase (fraction 5 [2])	35,922	Vir	C	Metabolism	P00354	7
	Junctional adhesion molecule A (fraction 3 [2])	32,518 (G)		M	Adhesion	Q9Y624	5
	Macrophage capping protein	38,518		C, N	Actin cytoskeleton	P40121	5
	Vacuolar ATP synthase subunit d	40,329		C, M	Vesicular acidification	P61421	5
	Fructose-1,6-bisphosphatase 1	36,683		C	Catabolism	P09467	3
	Biliverdin reductase A	33,428		C	Metabolism	P53004	5
	Malate dehydrogenase	36,295		C	Metabolism	P40925	3
	Poly(rC)-binding protein 1	37,498		N	Nuclear export	Q15365	3
	26S proteasome non-ATPase regulatory subunit 14	34,577		C, N	UPS	O00487	2
	Actin-related protein 2/3 complex subunit 1B (p41-ARC)	40,819		C	Actin cytoskeleton	O15143	2
	F-actin capping protein alpha-1 subunit (CapZ alpha-1)	32,923		C	Actin cytoskeleton	P52907	2
	Gi2 alpha	41,548	Exo	C	Signaling	Q6B6N3	2
	N-Acetylglucosamine kinase	37,244		C	Carbohydrate metabolism	Q9UJ70	2
	Protein XRP2	39,641		?	?	O75695	2
	Transcriptional activator protein PUR-alpha	34,911		N	Transcription	Q00577	2
	1-Phosphatidylinositol-4,5-bisphosphate phosphodiesterase-like 4	129,725		?	Lipid signaling	O75038	2
	Erythroid membrane-associated protein	52,589		M, C	Adhesion	Q7Z3X0	2
	Polypyrimidine tract-binding protein 1 (PTB1)	57,221		C	Splicing, translation	P26599	2
9 (43–48)	**Beta actin (fractions 8 [1], 10 [1], 11 [1], and 14 [1])**	41,736	Exo, Vir	C	Actin cytoskeleton	P60709	5
	Alpha-actin-2 (fractions 1 [2], 3 [2], 4 [3], 6 [4],7 [2], 8 [5], 13 [2], 14 [3], 15 [4], and 16 [2])	42,009	Exo, Vir	C	Actin cytoskeleton	P62736	5
	2′,3′-Cyclic nucleotide 3′-phosphodiesterase (fraction 7 [2])	47,578		M	Signaling	P09543	4
	HLA class A (fractions 8 [5], 10 [2], 12 [2])	40,846 (G)	Vir	M	Antigen presentation	P30443	3
	HLA class B (fraction 8 [2])	40,331 (G)	Exo, Vir	M	Antigen presentation	P30460	4
	HLA class C	40,710 (G)	Vir	M	Antigen presentation	P10321	2
	CD82 (fractions 10 [2] and 11 [3])	29,625 (G)	Exo	M	Signaling	P27701	2
	Titin (cellular fragment)[i]	3816,262		C	Contraction	Q8WZ42	2
	Phosphoglycerate kinase 1 (PRP2)	44,483		C	Metabolism	P00558	2
	Complement C4b	75,437		S	Cell lysis	P01028	2
10 (48–56)	**6-Phosphogluconate dehydrogenase**	53,008		C	Metabolism	P52209	10
	LAP3 protein	56,136		?	?	Q6IAM6	6
	GDP dissociation inhibitor beta (Rab GDIb)	50,663	Exo	C, M	Regulation of Rab targeting	P50395	6
	eEF1A (elongation factor-1 alpha) (fractions 3 [2], 5 [2], 6 [4], 7 [2], 8 [5], 12 [3], 13 [3], 15 [3], 16 [2])	50,141	Exo, Vir	C	Translation	Q05639	5
	Alpha-2-HS-glycoprotein (fetuin-A) (fractions 11 [2], 12 [3], and 16 [2])	39,324 (G)		S	Endocytosis	P02765	3
	Serine protease HTRA1	51,287		S	Protease	Q92743	5
	Vimentin (fractions 5 [2] and 9 [2])	53,520		C	IF cytoskeleton	P08670	5
	Annexin A11	54,390		C, N	?	P50995	4
	Disulfide isomerase ER-60	56,782		ER	Protein folding	P30101	4

Continued on facing page

TABLE 1—*Continued*

Fraction (size range in kDa)	Protein name[b]	Mol mass (Da)[c]	Particle[d]	Location[e]	Function/structure in which protein is involved[f]	Accession no.[g]	No. of peptides
	Thymidine phosphorylase (TdRPase)	49,955		C	Metabolism	P19971	4
	Adenylyl cyclase-associated protein 1 (CAP1)	51,542		M	Actin-RNA-binding regulation	Q01518	3
	Alpha-enolase (fraction 8 [3])	47,038		C, M	Multiple function	P06733	3
	Coronin-1A	51,026		C	Actin cytoskeleton	P31146	3
	CD14	40,076 (G)		M	LPS receptor	P08571	3
	CD147	42,200 (G)		M	Adhesion	P35613	2
	CD48	27,683 (G)		M	Signaling	P09326	2
	HU-K4 (fractions 11 [2], 12 [2], and 13 [2])	48,771		?	?	Q92853	2
	Rho-GTPase-activating protein 1	50,436		C	Signaling	Q07960	2
	Alpha-1,3-mannosyl-glycoprotein 2-beta-*N*-acetylglucosaminyltransferase	50,862		G	Glycosylation	P26572	2
	ATP synthase beta chain	56,560		Mi	Metabolism	P06576	2
	TCP-1-beta	57,357		C	Protein folding	P78371	2
	Tubulin alpha-1	49,924	Exo	C	Microtubules	P68366	2
	Vacuolar ATP synthase subunit B	56,501		C	Endocytosis	P21281	2
	CD2/LFA-2 (fractions 2, 5, 7, 14 [1], and 16 [1])	39,439 (G)	Vir	M	Signaling	P06729	1
	Heat shock 40-kDa protein 4	44,868		M	Protein folding	P31689	5
	Hsc70-interacting protein (HIP)	41,332		C	Protein folding	P50502	3
	Actin-like protein 3 (ARP3)	47,371		C	Actin cytoskeleton	P61158	2
	K-glypican	62,412		M	Adhesion	O75487	2
	Pigment epithelium-derived factor (PEDF)	46,342		S	Differentiation	P36955	2
	Radixin	68,564		M	Cytoskeleton	P35241	3
	Brain acid soluble protein 1 (BASP1, NAP22)	22,562		M	Actin cytoskeleton	P80723	2
	Ifapsoriasin	248,073		C	IF cytoskeleton	Q5D862	2
	Solute carrier family 12 member 7	119,150		M	Ion transporter	Q9Y666	2
11 (56–64)	**Pyruvate kinase (fractions 8 [3], 10 [4], 12 [15], 14 [2], and 15 [3])**	57,805		C	Metabolism	P14618	9
	L-Plastin (lymphocyte cytosolic protein 1)	70,289		C	Actin cytoskeleton	P13796	9
	EHD4 (fractions 10 [3] and 12 [5])	61,175		C	Vesicle trafficking	Q9H223	4
	Copine III (Ca^{2+} kinase)	60,130		M	Membrane organization	O75131	5
	Carboxypeptidase M (fraction 12 [3])	50,514 (G)		M	Extracellular protease	P14384	2
	Protein kinase C (fraction 12 [4])	55,739		C	Vesicular transport	Q9UNF0	2
	Gamma-glutamyltransferase 1 (fraction 13 [2])	61,382		M	Redox control	P19440	2
	LIR-D1	55,903		M	Adhesion	Q8NG09	2
	Lipid transfer protein II (fraction 13 [2])	54,739		S	Phospholipid transport	P55058	3
	Moesin (fractions 8 [3] and 10 [6])	67,689		C	Membrane-organizing	P26038	6
	75-kDa glucose-regulated protein (GRP75)	73,680		Mt	Protein folding	P38646	5
	78-kDa glucose-regulated protein (GRP78)	72,333		ER	Protein folding	P11021	4
	Annexin A6	75,742		C, M	Signaling	P08133	3
12 (64–70)	**Membrane matrix metalloproteinase-14**	65,883		M	Membrane organization	P50281	6
	Hsc70 (fractions 9 [2] and 11 [14])	70,898	Exo, Vir	C	Protein folding	P11142	6
	Hsp70-2 (fractions 9 [2] and 11 [6])	70,021	Vir	C	Protein folding	P54652	4
	Hsp70-1 (fractions 6 [2] and 11 [12])	70,052	Vir	C	Protein folding	P08107	3
	Hsp70-1L (fractions 6 [2] and 11 [5])	70,375		C	Protein folding	P34931	2
	CD58 (fractions 12 [2] and 13 [2])	28,147 (G)		M	Adhesion, signaling	P19256	2
	CD84	36,871 (G)		M	?	O15430	2
	Actin interacting protein 1	66,062		C	Actin cytoskeleton	O75083	2
	Hsp60	61,055		C	Protein folding	P10809	3
	Kindlin-3 (fractions 2 [2], 5 [2], 6 [5], 8 [10], 15 [3], 16 [2])	75,952		C	Cytoskeleton	Q86UX7	8
	Thyroxine-binding globulin	46,325		S	Thyroxine transport	P05543	3
	Tyrosine-protein phosphatase (SHP-1)	67,561		C	Signaling	P29350	3
	Catalase	59,625		C	Redox control	P04040	2
	LAMP-1 (CD107a) (fractions 14 [2] and 15 [2])	44,773 (G)		M	Endocytic trafficking	P11279	2
13 (70–80)	**Hsp90 (fractions 15 [2] and 16 [3])**	83,133	Exo	C	Protein folding	P08238	10
	CD98	57,945 (G)		M	Amino acid transport	P08195	3
	CD54 (ICAM-1) (fraction 14 [4])	57,825 (G)		M	Adhesion	P05362	3
	Quiescin Q6, isoform a (QSCN6)	82,578		?	?	O00391	4
	Endopeptidase-2	84,368		M	Protease	Q16819	3
	Rho GTPase activating protein 18	74,947		?	?	Q8N392	2
	ALB protein (fractions 10 [2], 11 [5], 12 [3], 14 [2], and 15 [2])	71,705		?	?	Q5D0D7	2
	Gelsolin	85,697		C	Actin cytoskeleton	P06396	9
	Periostin	93,332		S	Adhesion	Q15063	5
	Hsp89-alpha-delta-*N*	63,252		?	Protein folding	O75322	4
	Signal transducer and activator of transcription 1 (STAT1)	87,335		C	Signaling	P42224	4
	Matriptase (MT-SP1)	94,770		M	Protease	Q9Y5Y6	4
	gp91-phox	65,205		M	pH regulation	P04839	2
	Tumor necrosis factor alpha-induced protein 3	89,614		C, N	Signaling	P21580	3
	26S proteasome regulatory subunit RPN1	100,200		C, N	UPS	Q13200	2
	CDC48/p97	89,191		C, N	Vesicle trafficking	P55072	2
	Vps35 (human homolog)	91,707		C, M	Vesicle sorting	Q96QK1	2

Continued on following page

TABLE 1—*Continued*

Fraction (size range in kDa)	Protein name[b]	Mol mass (Da)[c]	Particle[d]	Location[e]	Function/structure in which protein is involved[f]	Accession no.[g]	No. of peptides
14 (80–100)	**CD18 (integrin beta-2) (fraction 13 [4])**	84,790 (G)	Exo, Vir	M	Adhesion	P05107	19
	CD36 (fraction 13 [2])	52,922 (G)		M	Adhesion	P16671	7
	CD43 (leukosialin) (fractions 5 [2] and 13 [2])	40,322 (G)	Vir	M	Signaling	P16150	1
	CD44 (fractions 4 [3], 5 [3], 6 [2], 11 [7], and 13 [3])	81,214 (G)	Vir	M	Adhesion	P16070	3
	CD61 (integrin beta-3)	87,214		M	Adhesion	P05106	3
	CD49c (integrin alpha-3)	118,698		M	Adhesion	P26006	2
	CD86	37,696 (G)		M	T-cell regulation	P42081	2
	CD276	57,235 (G)		M	T-cell regulation	Q5ZPR3	2
	CD315 (fraction 15 [4])	98,556		M	Signaling	Q9P2B2	4
	Na^+/K^+ ATPase 1 (fraction 15 [2])	112,896		M	Ion transport	P05023	10
	AIP-1/Alix (fractions 2 [2] and 12 [3])	96,023	Exo, Vir	C	LE trafficking	Q8WUM4	9
	Hexokinase-3	98,919		C	Microtubule motor	P52790	6
	94-kDa glucose-regulated protein (GRP94)	92,469		ER	Protein folding	P14625	5
	Elongation factor 2 (EF-2) (fraction 13 [6])	95,207		C	Translation	P13639	2
	Importin beta-1 (importin 90) (fraction 13 [2])	97,170		N, C	Nuclear shuttling	Q14974	2
	Vacuolar proton pump subunit 1	96,413		M	Endosome acidification	Q93050	2
	KIFC3 kinesin (fractions 3, 4, 5, 6, 10, and 16 [2])	77,866		C	Vesicle trafficking	Q9BVG8	1
	Putative helicase MOV-10 (fraction 12 [2])	113,671		?	?	Q9HCE1	5
	HEM-1	128,215		M	?	P55160	4
	Vinculin	123,668		M	Actin cytoskeleton	P18206	3
	Fibulin-1	77,261		S	Adhesion	P23142	2
	Inter-alpha-inhibitor heavy chain 2 (fractions 12 [2], 13 [2], 14 [2], and 16 [2])	106,436		S	Hyaluronan binding	P19823	2
15 (100–130)	**CD11b (Mac-1, integrin alpha-M) (fraction 11 [2])**	27,178 (G)	Exo, Vir	M	Adhesion	P11215	11
	CD13 (fraction 14 [2])	109,380		M	Signaling	P15144	10
	CD11c (fractions 14 [2] and 16 [2])	127,887		M	Adhesion	P20702	8
	CD29 (integrin beta-1)	884,654 (G)		M	Adhesion	P05556	5
	CD18 (integrin beta-1 chain)	88,465 (G)	Exo, Vir	M	Adhesion	P05556	2
	CD49e (fibronectin receptor alpha subunit)	114,536		M	Adhesion	P08648	2
	CD51 (vitronectin receptor alpha subunit)	116,052		M	Adhesion	P06756	2
	CD304 (neurophilin-1) (fractions 14 [3] and 16 [2])	103,120		M	Signaling receptor	O14786	2
	EMILIN-2	115,616		S	Adhesion	Q9BXX0	6
	Thrombospondin-1	129,413		?	Adhesion	P07996	2
	Myoferlin (fraction 16 [3])	234,709		M	Membrane organization	Q9NZM1	6
	Protein tyrosine phosphatase receptor type C (PTPRC)	131,130		M	Signaling	Q5T5R0	4
	Cytoplasmic FMR1 interacting protein isoform 1	145,182		C	Translation/RNA location	Q7L576	3
	Cytoplasmic FMR1 interacting protein isoform 4	94,523		C	?	Q6ZSX1	2
	Type 3 inositol 1,4,5-trisphosphate receptor	304,038		ER	Signaling	Q14573	2
	Nicastrin	78,411		M	Protease	Q92542	2
	Ras GTPase-activating-like protein (IQGAP1) (fraction 14 [2])	189,252		M	Actin cytoskeleton	P46940	2
16 (130–280)	**Fibronectin**	262,607		S, M	Adhesion	P02751	17
	Clathrin heavy chain 1 (fractions 3 [3], 8 [6], 10 [6], 11 [7], 12 [8], 13 [11], 14 [15], and 15 [31])	191,614		C	Endocytosis	Q00610	12
	CD148	145,927 (G)		M	Signaling	Q12913	2
	CD169 (sialoadhesin)	182,624		M	Adhesion	Q9BZZ2	6
	CD205	198,271		M	Endocytosis	O60449	2
	Tenascin-C	240,866		S	Adhesion	P24821	3
	Talin-1 (fractions 14 [2] and 15 [3])	269,767		M	Cytoskeketon membrane	Q9Y490	19
	Complement C3 (fraction 14 [2])	187,164		S	Cell lysis	P01024	2
	NPC-1 (fraction 15 [1])	142,167		C	LE/cholesterol trafficking	O15118	1
	Dermcidin	11,284		S	Antimicrobial reaction	P81605	2
17 (>280)	**Filamin A (FLNa)**	280,759		S	Actin cytoskeleton	P21333	17
	Plectin 1 (PLTN)	531,732		C	IF cytoskeleton	Q15149	4

[a] The CID spectra were compared against those of the EMBL nonredundant protein database by using SEQUEST (ThermoElectron, San Jose, CA). Only those peptides having cross-correlation (X_{corr}) cutoffs of 1.9 for $[M + H]^{1+}$, 2.2 for $[M + 2H]^{2+}$, and 3.5 for $[M + 3H]^{3+}$ and with delta cross-correlation scores (ΔCn) of at least 0.09 (65) were considered. Proteins were identified at least by two peptides, either unique peptides in the same fraction or independent observations in different fractions. These SEQUEST criteria thresholds have been determined previously to result in a 95% confidence level in peptide identification (77).

[b] Alternative names are provided in parentheses. Proteins whose observed mass falls within the expected molecular mass range of their fraction are shown in bold. Peptides from a given protein found in more than one fraction are indicated in parentheses with the other fraction numbers in which it was observed. The number of peptides found in the secondary fractions is indicated in brackets.

[c] Theoretical molecular mass for the primary translation product calculated from DNA sequences protein. Glycosylated proteins are indicated by a G. Proteins with a processed cellular form are indicated by a P.

[d] Proteins previously found in virions (Vir) or exosomes (Exo) are indicated.

[e] The locations of the protein are indicated as follows: C, cytoplasmic (can include intracellular vesicles); M, plasma membrane; N, nuclear; S, secreted; ER, endoplasmic reticulum; G, Golgi; P, peroxisomal; and ?, unknown.

[f] Abbreviations: UPS, ubiquitin/proteasome system; IF, intermediate filament; LE, late endosome; ER, endoplasmic reticulum; Reg., regulation; Red/Ox, reduction oxidation; and ?, unknown.

[g] Accession numbers for UniProt (accessible at http://www.pir.uniprot.org/search/textSearch.shtml).

[h] eEF1A (formerly named elongation factor-1 alpha) (12) fragments produced by HIV-1 protease (11, 51).

[i] A 47-kDa truncated version of titin of unknown function was detected in immunoblots of monocyte-derived macrophage cultures (data not shown).

from each gel slice was analyzed by MALDI-TOF MS prior to LC-MS/MS analysis. The MALDI-TOF MS data confirmed that the digested samples contained high-quality peptides and provided a good estimate of the relative protein concentrations in these samples. Therefore, a portion of the peptide samples that were extracted from the gel bands was analyzed by μRPLC-MS/MS. The results showed that all fractions of the gel contained statistically significant peptide identifications (those proteins identified with more than one peptide at a confidence level greater than 97%). A μRPLC-MS/MS analysis of fractions 7 and 8 from the parallel preparative-scale SDS-PAGE analysis of the CD45-depleted uninfected control preparation produced no statistically significant peptide identifications (data not shown). In contrast, the same fractions produced many peptides in the virus sample analysis (Table 1); thus, the proteins identified in the CD45-depleted virus samples appear to be from the virus and not from contaminating vesicle-associated proteins.

The tandem mass spectra were compared against spectra of the EMBL nonredundant human protein database by using a SEQUEST search program. After filtering the results based on X_{corr} (cutoffs of 1.9 for $[M + H]^{1+}$, 2.2 for $[M + 2H]^{2+}$, and 3.5 for $[M + 3H]^{3+}$) and ΔC_n (at least 0.09) values, the peptide identifications were segregated into cellular and viral proteins: the 253 unique cellular proteins are shown in Table 1 and the expected set of viral proteins is shown in Table 2. The implications and caveats on these findings are presented in Discussion below.

Immunoblot analysis of virions. While our μRPLC-MS/MS analysis found a large number of proteins, it failed to detect the CD63 protein, a marker for the late endosomal/MVB system that was previously found in macrophage-produced HIV-1 (45, 54). Failure to identify a protein by μRPLC-MS/MS peptide analysis does not conclusively demonstrate that the protein is not present in the analyzed sample, since the absence of identifiable peptides can be due to several technical factors, especially for highly glycosylated proteins such as CD63. To determine if CD63 was present in our MDM-derived HIV-1 preparations, CD45-depleted preparations from uninfected and infected cultures (equal amounts by volume approximately 200 ng $p24^{CA}$ in the virion sample) were examined by immunoblot analysis. The results revealed that the CD45-depleted virion preparations did indeed contain CD63, confirming that CD63 is present in HIV-1 virions produced from MDM, while there was no signal from the matched CD45-depleted uninfected cell sample (Fig. 4).

Tsg101, a late endosomal sorting protein that is essential for viral budding, has been found in HIV-1 virions produced from HeLa cell and T-cell lines (14, 22, 75). However, we did not find any Tsg101 peptides by our μRPLC-MS/MS analysis in fraction 9, where the full-length protein should migrate in the gel (44 kDa). However, we did find two peptides in fraction 5 that spans 20 to 24 kDa. To confirm the presence of this important protein, we carried out an immunoblot analysis of CD45-depleted preparations from infected and uninfected MDM (equal amounts by volume with approximately 200 ng $p24^{CA}$ in the virion sample). The results revealed a band of 43 kDa that corresponds to full-length Tsg101, as well as a 22-kDa band that confirms the presence of a fragment of Tsg101 as indicated by the peptide sequences in fraction 5. Since this fragment was not detected in MDM cellular lysates (data not shown), it might be a protease cleavage HIV-1 product of some of the Tsg101 incorporated into virions. Other cellular proteins in the virion are known to be cleaved by HIV-1 protease (11, 51, 52, 70). In contrast to the virion sample, the CD45-depleted sample from a parallel, uninfected cell culture contained no detectable Tsg101 signal (Fig. 4). These data confirm that both full-length and truncated forms of Tg101 are present in MDM-derived HIV-1 virions.

TABLE 2. Viral proteins

Fraction (size in kDa)	Protein name[a]	No. of peptides
1 (5–7)	**Pol TF ($p6^{pol}$, p6*, preprotease)**	1
	$gp41^{TM}$	1
	$gp120^{SU}$	2
2 (8–11)	**Pol ^{TF} ($p6^{pol}$, p6*, preprotease)**	2
	$p7^{NC}$	2
	$p6^{Gag}$	2
	RNase H	1
	$p17^{MA}$	4
3 (11–16)	**$p24^{CA}$**	3
	IN	2
	Tat	1
	RNase H	2
4 (16–20)	**$p17^{MA}$**	18
	Nef	1
5 (20–24)	**$p17^{MA}$**	7
6 (24–29)	**$p24^{CA}$**	8
	Nef	1
7 (29–34)	**IN**	1
	$P17^{MA}$	6
	$P24^{CA}$	3
9 (43–48)	**$gp41^{TM}$**	2
	$gp120^{SU}$	3
10 (48–56)	**$Pr55^{Gag}$ ($p17^{MA}$)**	2
	$Pr55^{Gag}$ ($p24^{CA}$)	2
	RT	1
11 (56–64)	**$Pr55^{Gag}$ ($p17^{CA}$)**	1
	$Pr55^{Gag}$ ($p24^{CA}$)	1
	$gp41^{TM}$	5
12 (64–70)	**RT**	1
	Vif	2
13 (70–80)	**Nef**	1
14 (80–100)	Nef	2
15 (100–130)	**$gp120^{SU}$**	3

[a] Proteins whose observed mass falls within the expected molecular mass range of their fractions are shown in bold. The $Pr55^{Gag}$ peptides detected in fractions 10 and 11 are indicated in parentheses. Pol TF, polymerase transframe; RT, reverse transcriptase; IN, integrase.

Env content of MDM-derived HIV-1. Previously, we found that HIV-1 and simian immunodeficiency virus virions produced from various T-cell lines in which the virus assembles on the cell surface contain between 7 and 14 Env trimers per virion (10, 78). To evaluate whether the alternative MVB-based assembly and budding mechanism used by HIV-1 in macrophages alters the incorporation of Env into virions, the proteins in an MDM-derived HIV-1 preparation that was density gradient-purified twice were separated and collected into fractions by HPLC (Fig. 5). SDS-PAGE gel analysis of the fractions containing $p24^{CA}$ (fractions 38 to 44) showed an intense $p24^{CA}$ band, while those containing $gp120^{SU}$ (fractions 27 to 30) showed only a small amount of signal for $gp120^{SU}$ relative to the large amounts of cellular proteins. Quantitative

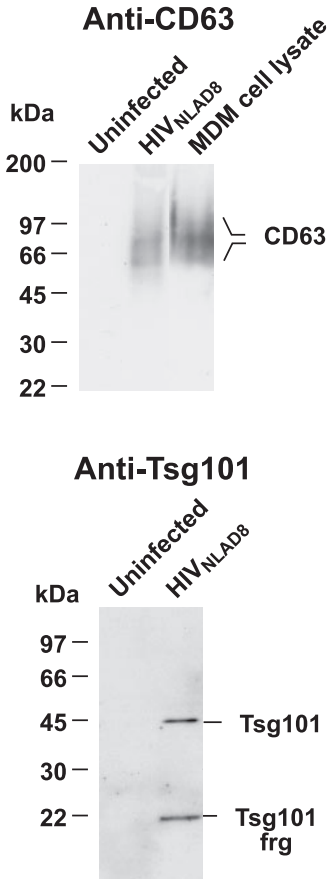

FIG. 4. CD63 and Tsg101 immunoblots of MDM-derived HIV-1. Immunoblots of virion preparations (equal amounts by volume with approximately 200 ng $p24^{CA}$ in the virion sample) isolated from parallel uninfected and HIV-1_{NLAD8}-infected MDM cultures are shown. The samples are identified above their respective lanes. The antibody or antiserum used is indicated above each blot. For the CD63 immunoblot, a lane containing a cell lysate control from uninfected MDM (lysate from 5×10^5 cells) is included. frg, fragment.

amino acid analysis to measure $gp120^{SU}$ content was therefore not feasible. To determine the relative contents of Gag and Env in virions, we quantitated the amounts of both Gag ($p24^{CA}$) and Env ($gp120^{SU}$) in MDM-produced virion preparations by fluorescence-based quantitation (39). SDS-PAGE gels of virus samples and serial dilutions of purified protein standards were stained first with SYPRO Pro-Q Emerald, a fluorescent dye that detects glycoproteins, and the $gp120^{SU}$ signal was measured. The proteins in the gel were then stained with the fluorescent dye SYPRO Ruby, which reacts with all proteins, and the amount of $p24^{CA}$ present was determined. A merged image of a representative gel is presented in Fig. 5B. The masses of $p24^{CA}$ and $gp120^{SU}$ in the virion samples were then calculated by interpolation of integrated pixel densities for the test samples onto standard curves obtained from a dilution series of calibrated protein standards (Fig. 5B; Table 3). Based on these data, the molar Gag-to-Env ratio was 39 to 1. This corresponds to an average of 12 Env trimers per MDM-derived HIV particle based on an estimated 1,400 Gag molecules per particle. This is the value that we previously have determined by direct enumeration of trimers on individual

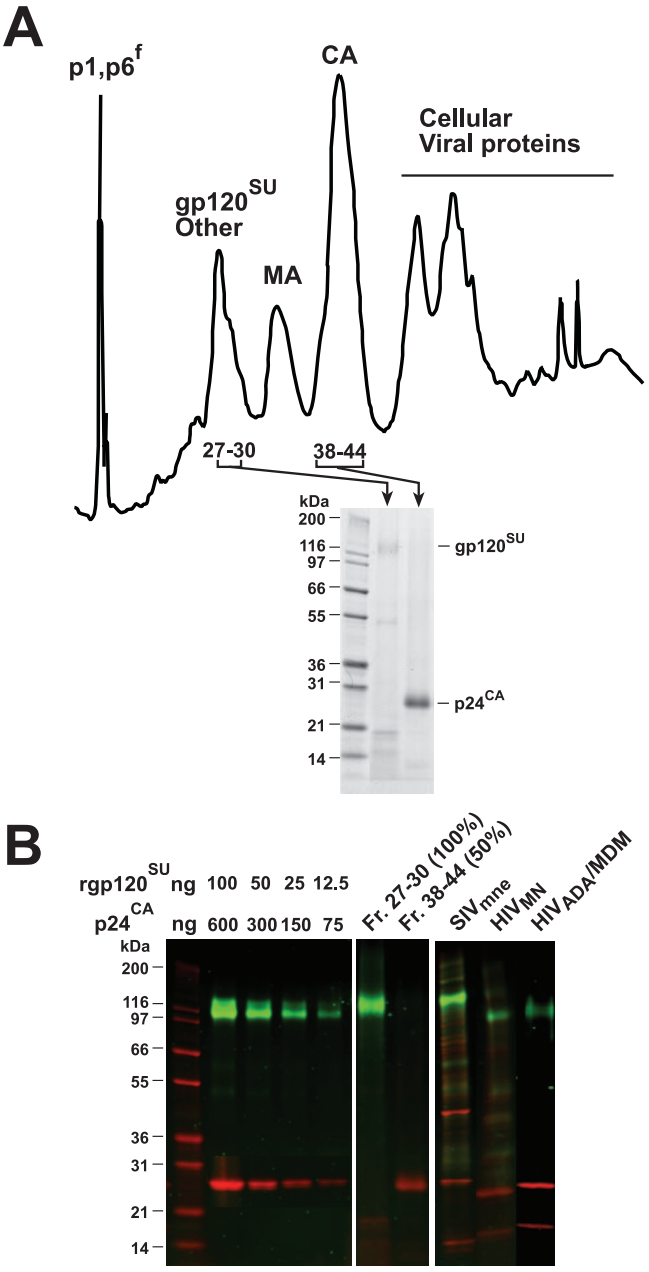

FIG. 5. Env content analysis of MDM-derived HIV-1. (A) An HPLC chromatogram (A_{206}) of HIV-1_{ADA} produced from MDM is shown. Reversed-phase HPLC of denatured virions was performed as described in Materials and Methods. Viral protein peaks (identified by SDS-PAGE gels) are labeled above the chromatograph, and Coomassie blue-stained SDS-PAGE gel analysis of pertinent corresponding fractions is shown below, with positions of the molecular mass markers denoted at the left. (B) A two-dye SYPRO-stained SDS-PAGE gel is shown. Samples are identified above their respective lanes. For the recombinant $gp120^{SU}$ ($rgp120^{SU}$) and purified $p24^{CA}$ standards, the amount of material loaded in each lane (in ng) is indicated above each lane. The relative loads, by volume, for the HPLC fractions are indicated in parentheses on the lane labels. The images of these standards have been digitally overlaid and merged for presentation purposes. The relative intensities of these images have not been altered. The positions of molecular mass markers are denoted at the left. $p6^f$, an HIV protease cleavage fragment of p6; Fr., fraction.

TABLE 3. Quantitation of Env and Gag in virion preparations

Virus preparation	Amt (pmol) of:		Amt of CA/amt of gp120	Env molecules/ virion in:	
	CA[a]	gp120[b]		Two-color assay[c]	Previous report[d]
HIV-1/MDM[e]	24	0.62	39	12	ND
HIV-1_{MN}/clone 4	5.5	0.09	63	7	6
SIV_{mne}/E11S	3.8	0.53	7.2	67	60

[a] Calculated from the ng of protein detected by SYPRO orange assay.
[b] Calculated from the ng of protein detected by SYPRO green assay.
[c] Calculations using 1,400 Gag molecules per virion as estimated by Zhu et al. (78).
[d] Previously determined number of Env molecules per virion from amino acid analysis (1,400 Gag molecules per virion) (10). ND, not determined.
[e] Produced from pooled harvests of infected MDM on six-well hydrogel-treated plates ($\sim 10^7$ cells per well).

virions by electron tomography combined with biochemical quantitation of Gag/Env ratios (78). However, by comparing in vitro-produced Gag particles to immature virions, another group has estimated that there are 5,000 Gag molecules per virion (5). While there currently is no clear resolution between the two methods, we favor our direct approach because the virions are produced under native conditions. The number of Env trimers quantified using this method also correlates well with the Gag/Env stoichiometry of other retroviruses (53, 74). For comparison, the two-dye fluorescent analysis of the well-characterized control virus preparations HIV-1_{MN}/H9 clone 4 and SIV_{mne}/HuT-78 cl.E11S yielded results (Table 3) that showed excellent agreement with previous results obtained by alternative methods (6:1 and 60:1 trimers per 1,400 Gag molecules, respectively [10, 78]).

DISCUSSION

The proteomic analysis of HIV-1 virions produced from monocyte-derived macrophages presented here reveals many new proteins not previously described in HIV-1 virions. These proteins are components of a wide variety of cellular systems. Since viruses rely heavily on cellular systems for their replication, these proteins provide potential clues for viral biology. Of the 253 unique proteins identified, 33 were proteins previously found in virions produced from nonmacrophage cells (Table 1) (49, 71). However, most of the proteins (i.e., 220) had not been previously identified in HIV-1 particles. Many of the observed proteins were found in gel fractions corresponding to their expected size, as deduced from their amino acid sequence. In addition, other proteins, especially the glycosylated proteins, were found in fractions with higher molecular mass than the protein sequence. Other posttranslational modifications, such as phosphorylation and ubiquitination, might also cause proteins to migrate more slowly than expected and be found in higher-molecular-mass bands on the SDS-PAGE gels. The presence of ubiquitin in several higher-molecular-mass fractions (fractions 4, 6, 8, 10, 12, and 15) is consistent with the potential presence of ubiquitin-conjugated proteins in these regions. In contrast, some proteins migrated at a faster rate, reflecting a lower molecular mass than expected for the full-length protein. In some cases, this might be due to HIV-1 protease cleaving cellular proteins (70). For example, eEF1A (formerly elongation factor-1 alpha), which has been previously found in HIV-1 virions in a full-length (53-kDa) form and as a 30-kDa C-terminal-cleaved fragment, was detected in both the 29- to 34-kDa and 34- to 43-kDa fractions (11, 51). Also, immunoblot analysis demonstrated the presence of a truncated form of Tsg101 in virions. A molecular mass lower than expected might also be due to cellular proteins being expressed in truncated forms through alternative splicing of message or posttranslational cleavage by cellular proteases inside the cell. One surprise on our list was a titin peptide in fraction 9 (43 to 48 kDa). However, immunoblot analysis of MDM cell lysate demonstrated the presence of a 47-kDa species of what is normally a 3-MDa protein (L. V. Coren and D. E. Ott, unpublished results). The significance or function of this truncated titin in MDM cells is not known.

Cellular proteins may be incorporated into virions as bystanders, simply by being fortuitously present at the site of budding. Alternatively, such proteins as Tsg101 (fraction 5) and AIP1 (Alix; fractions 2, 12, and 14), which interact with Gag to help form the virion and assist in the budding process (13, 44, 64, 75) might be incorporated because they are active participants in different stages of the viral replication cycle,. Lastly, cellular proteins preferentially incorporated into virions may influence viral biology and pathogenesis, as has been shown for integrins, which can increase infectivity (4, 66), and HLA class II proteins, the presence of which on virions has been associated with an induction of increased levels of apoptosis in vitro (19). Based on these precedents, identification of additional cellular proteins incorporated into virions may provide useful insights into viral biology.

The virion preparations described herein contained proteins from several important cytoplasmic systems, including the actin cytoskeleton, microtubules, ubiquitin/proteasomes, translation, protein chaperones, signal transduction, endosome/exosome, and metabolism. In addition, surface proteins associated with cell signaling, adhesion, and antigen presentation were identified. However, at present, the relevance of these proteins to viral biology is not clear. While all of these proteins provide important possibilities for influencing viral function, the present observations represent a starting point. Further studies will be needed to determine the relevance of these host proteins to viral biology.

One of the current models for HIV-1 budding suggests that the viral components, especially Gag, assemble at either late endosome/MVB vesicles directly or at late endosomal/MVB-derived patches on the plasma membrane before budding (3, 7, 26, 29, 42, 46, 54, 55, 63, 75). In macrophages, immunoelectron microscopy for HIV-1 Gag and cellular markers indicates that the internal vesicles harboring HIV-1 are late endosomal/MVB structures (54). Our data support these observations; we found many common endosomal/MVB proteins in HIV-1 derived from macrophages, including HLA class II, actin, and actin-binding proteins, as well as tetraspanins, e.g., CD9 (fraction 6 and others), tetraspanin-14 (fraction 6), CD53 (fraction 8 and others), CD81 (fractions 2 and 5), CD82 (fractions 10 and 11), and the CD63 late endosome marker. A recent report by Nydegger et al. has found that HIV-1 assembles and buds at membrane regions that contains tetraspanins (CD9, CD63, CD81, and CD82), Vps28, and Tsg101 (47), proteins identified by our analyses.

One of the endosomal/MVB-associated proteins that we found in virions, annexin 2 (fractions 7, 8, and 9), is a cytoplasmic actin-binding protein, which translocates to the plasma membrane in stimulated cells (24). Annexin 2 tightly binds to a member of the S100 family of calcium-binding proteins, S100A10 (p11). Upon binding, annexin 2 and S100A10 form a heterotetramer which is capable of binding two membrane surfaces simultaneously, potentially promoting fusion events (38), and also plays a role in exocytosis (24). The S100A10 (fraction 2) protein was also detected by our analysis, suggesting that HIV-1 derived from MDM incorporates this complex. Other S100 family members were also detected in viral sample (fraction 2) and could play various roles in fusion and membrane organization (16, 38). Recently, annexin 2 was shown to participate in lipid raft organization, as well as docking and fusion of secretory granules with the plasma membrane (exocytosis) in neuroendocrine cells (9). The presence of annexin 2 in HIV-1 viral particles supports the idea that HIV-1 is exploiting endosomal/exosomal pathways. Recently, Ryzhova et al. have shown that annexin 2A binds Gag and that small interfering RNA-mediated depletion of this annexin prevents viral budding from cells (61), suggesting a role for this protein in HIV-1 assembly. Other less studied annexin family members (annexins A5 [fraction 7], A11 [fraction 10], and A6 [fraction 11]) were also identified by our analysis, but their function in the cell is still not clear (24).

In addition to annexins, proteins from other important vesicle trafficking systems were also present. Rab protein family members, which function mostly in vesicle transport (6), are present in MDM-derived HIV-1 (fraction 6). The NPC1 protein, a protein that transports cholesterol through the late endosomal system (33), was also observed (fraction 15 and 16), further supporting the idea that HIV-1 assembly occurs on MVB membranes in macrophages. The sorting of proteins within the cell is regulated by members of the Vps family (13, 14, 20, 22, 42, 44, 75). Our analysis found Tsg101 (the human ortholog of yeast Vps23; fraction 5 and immunoblot), Vps28 (fraction 6), Vps29 (fraction 5), and Vps35 (fraction 13). These proteins are involved in vesicle sorting, and Tsg101 and Vsp28 are both members of the ESCRT I complex which has been shown to be involved in virus budding from the cell (13, 44).

Besides markers of the endosomal compartment, several components of exosomes were also identified by our analysis. Our macrophage-produced viruses contained 26 out of 37 proteins previously observed by a proteomic analysis of exosomes from dendritic cells (68), further supporting the proposal that HIV-1 and exosomes use similar budding mechanisms in macrophages, with the virus exploiting the exosome budding pathway to release virions (28).

Apolipoprotein E (ApoE; fraction 8) is best known for its role in plasma cholesterol transport (for a review, see reference 41) but has also been implicated in immunoregulation and modulation of cell growth and differentiation (35, 40, 41) and was identified in our analysis. Macrophages express ApoE (40), although the levels of expression can vary widely (67). ApoE binds lipid membrane surfaces (62), so the presence of this secreted protein could be the result of binding to the virion surface. Macrophages also endocytose ApoE and recycle it back to the surface (30), raising the possibility that HIV-1 could acquire this protein in an exocytotic compartment, such as the late endosomal system in macrophages. The presence of ApoE on a HIV-1 could potentially facilitate virus entry, by targeting HIV-1 virions to low density lipoprotein receptor-expressing cells, such as monocytes (58).

The list of cellular proteins that we found by our μRPLC-MS/MS analysis is quite large, and several important caveats need to be considered when interpreting these data. First, these proteins were found in a population of virions, and it is unlikely that a single virion contains all of these proteins. In addition, HIV-1 is structurally very heterogeneous (5), so the amount and variety of cellular proteins in any particular virion could be quite different from those of another. Another consideration is that while the μRPLC-MS/MS analysis used here identified many proteins, others proteins (e.g., CD63) were not detected. This reflects the intrinsic difficulty in identifying proteins present in relatively small amounts within complex mixtures, even after gel fractionation. The scoring thresholds used in this study have been shown to provide a confidence level of greater than 97% in the identification of a protein by peptides (17, 56, 73, 77). While at this level of stringency, identification of even a single peptide constitutes solid evidence for the presence of the parent protein in the sample (73), we have presented only those proteins that yielded at least two peptides. Consequently, some proteins may have been excluded from by our μRPLC-MS/MS analysis due to the high-stringency thresholds employed.

Our μRPLC-MS/MS analysis of highly purified HIV-1 produced from infected MDM has identified numerous cellular proteins potentially involved in various aspects of virus replication, especially assembly. However, we also identified proteins whose presence in virions is difficult to interpret mechanistically based on current knowledge. Some proteins simply might be incorporated due to their relatively large amounts at the site of budding. Another explanation is that cellular proteins can have multiple and very different functions, including functions other than those for which they are best known (34). However, it is unlikely that all these unexpected proteins have multiple pertinent functions. While we have applied what we consider to be the best technology available to produce highly purified virions, removing contaminating proteins present (both soluble protein and those in vesicular particles), some of the proteins identified here could be simply adhered to the virions and not functionally incorporated into the particles. Even with this caveat, this proteomic analysis represents important data because it provides leads for further studies of the involvement of cellular proteins and pathways in the HIV-1 replication cycle. Such studies should provide additional information about the assembly and budding pathways used by HIV-1 in infected macrophages, raise interesting questions about the possible contributions of some of these virion-incorporated molecules in HIV-1 pathogenesis, and may point to potential targets for novel approaches to therapeutic intervention in HIV-1 infection.

ACKNOWLEDGMENTS

We thank B. Bohn, J. Miller, T. Ireland, M. Poore, and R. Imming for purified viruses and M. Jason de la Cruz for skilled electron microscope assistance.

This project has been funded in whole with federal funds from the National Cancer Institute, National Institutes of Health, under contract N01-CO-12400. The content of this publication does not neces-

sarily reflect the views or policies of the Department of Health and Human Services, nor does mention of trade names, commercial products, or organizations imply endorsement by the U.S. Government.

REFERENCES

1. **Bess, J. W., Jr., R. J. Gorelick, W. J. Bosche, L. E. Henderson, and L. O. Arthur.** 1997. Microvesicles are a source of contaminating cellular proteins found in purified HIV-1 preparations. Virology **230:**134–144.
2. **Bess, J. W., Jr., P. J. Powell, H. J. Issaq, L. J. Schumack, M. K. Grimes, L. E. Henderson, and L. O. Arthur.** 1992. Tightly bound zinc in human immunodeficiency virus type 1, human T-cell leukemia virus type 1, and other retroviruses. J. Virol. **66:**840–847.
3. **Booth, A. M., Y. Fang, J. K. Fallon, J. M. Yang, J. E. Hildreth, and S. J. Gould.** 2006. Exosomes and HIV Gag bud from endosome-like domains of the T cell plasma membrane. J. Cell Biol. **172:**923–935.
4. **Bounou, S., J. F. Giguere, R. Cantin, C. Gilbert, M. Imbeault, G. Martin, and M. J. Tremblay.** 2004. The importance of virus-associated host ICAM-1 in human immunodeficiency virus type 1 dissemination depends on the cellular context. FASEB J. **18:**1294–1296.
5. **Briggs, J. A., M. N. Simon, I. Gross, H. G. Krausslich, S. D. Fuller, V. M. Vogt, and M. C. Johnson.** 2004. The stoichiometry of Gag protein in HIV-1. Nat. Struct. Mol. Biol. **11:**672–675.
6. **Bucci, C., and M. Chiariello.** 2006. Signal transduction gRABs attention. Cell Signal. **18:**1–8.
7. **Cantin, R., S. Methot, and M. J. Tremblay.** 2005. Plunder and stowaways: incorporation of cellular proteins by enveloped viruses. J. Virol. **79:**6577–6587.
8. **Chapman, J. R.** 2000. Mass spectrometry of protein and peptides. Humana Press, Totowa, N.J.
9. **Chasserot-Golaz, S., N. Vitale, E. Umbrecht-Jenck, D. Knight, V. Gerke, and M. F. Bader.** 2005. Annexin 2 promotes the formation of lipid microdomains required for calcium-regulated exocytosis of dense-core vesicles. Mol. Biol. Cell **16:**1108–1119.
10. **Chertova, E., J. W. Bess, Jr., B. J. Crise, I. R. Sowder, T. M. Schaden, J. M. Hilburn, J. A. Hoxie, R. E. Benveniste, J. D. Lifson, L. E. Henderson, and L. O. Arthur.** 2002. Envelope glycoprotein incorporation, not shedding of surface envelope glycoprotein (gp120/SU), is the primary determinant of SU content of purified human immunodeficiency virus type 1 and simian immunodeficiency virus. J. Virol. **76:**5315–5325.
11. **Cimarelli, A., and J. Luban.** 1999. Translation elongation factor 1-alpha interacts specifically with the human immunodeficiency virus type 1 Gag polyprotein. J. Virol. **73:**5388–5401.
12. **Clark, B. F. C., M. Grunberg-Manago, N. K. Gupta, J. W. B. Hershey, A. G. Hinnebusch, R. J. Jackson, U. Maitra, M. B. Matthews, W. C. Merrick, R. E. Rhoads, N. Sonenberg, L. L. Spremulli, H. Trachsel, and H. O. Voorma.** 1996. Prokaryotic and eukaryotic translation factors. Biochimie **78:**1119–1122.
13. **Demirov, D. G., and E. O. Freed.** 2004. Retrovirus budding. Virus Res. **106:**87–102.
14. **Demirov, D. G., A. Ono, J. M. Orenstein, and E. O. Freed.** 2002. Overexpression of the N-terminal domain of TSG101 inhibits HIV-1 budding by blocking late domain function. Proc. Natl. Acad. Sci. USA **99:**955–960.
15. **Denzer, K., M. J. Kleijmeer, H. F. Heijnen, W. Stoorvogel, and H. J. Geuze.** 2000. Exosome: from internal vesicle of the multivesicular body to intercellular signaling device. J. Cell Sci. **113:**3365–3374.
16. **Donato, R.** 2003. Intracellular and extracellular roles of S100 proteins. Microsc. Res. Tech. **60:**540–551.
17. **Elias, J. E., W. Haas, B. K. Faherty, and S. P. Gygi.** 2005. Comparative evaluation of mass spectrometry platforms used in large-scale proteomics investigations. Nat. Methods **2:**667–675.
18. **Esser, M. T., J. W. Bess, Jr., K. Suryanarayana, E. Chertova, D. Marti, M. Carrington, L. O. Arthur, and J. D. Lifson.** 2001. Partial activation and induction of apoptosis in $CD4^+$ and $CD8^+$ T lymphocytes by conformationally authentic noninfectious human immunodeficiency virus type 1. J. Virol. **75:**1152–1164.
19. **Esser, M. T., D. R. Graham, L. V. Coren, C. M. Trubey, J. W. Bess, Jr., L. O. Arthur, D. E. Ott, and J. D. Lifson.** 2001. Differential incorporation of CD45, CD80 (B7-1), CD86 (B7-2), and major histocompatibility complex class I and II molecules into human immunodeficiency virus type 1 virions and microvesicles: implications for viral pathogenesis and immune regulation. J. Virol. **75:**6173–6182.
20. **Freed, E. O.** 2002. Viral late domains. J. Virol. **76:**4679–4687.
21. **Freed, E. O., G. Englund, and M. A. Martin.** 1995. Role of the basic domain of human immunodeficiency virus type 1 matrix in macrophage infection. J. Virol. **69:**3949–3954.
22. **Garrus, J. E., U. K. von Schwedler, O. W. Pornillos, S. G. Morham, K. H. Zavitz, H. E. Wang, D. A. Wettstein, K. M. Stray, M. Cote, R. L. Rich, D. G. Myszka, and W. I. Sundquist.** 2001. Tsg101 and the vacuolar protein sorting pathway are essential for HIV-1 budding. Cell **107:**55–65.
23. **Gelderblom, H. R.** 1991. Assembly and morphology of HIV: potential effect of structure on viral function. AIDS **5:**617–638.
24. **Gerke, V., C. E. Creutz, and S. E. Moss.** 2005. Annexins: linking Ca2+ signalling to membrane dynamics. Nat. Rev. Mol. Cell Biol. **6:**449–461.
25. **Gluschankof, P., I. Mondor, H. R. Gelderblom, and Q. J. Sattentau.** 1997. Cell membrane vesicles are a major contaminant of gradient-enriched human immunodeficiency virus type-1 preparations. Virology **230:**125–133.
26. **Goff, A., L. S. Ehrlich, S. N. Cohen, and C. A. Carter.** 2003. Tsg101 control of human immunodeficiency virus type 1 Gag trafficking and release. J. Virol. **77:**9173–9182.
27. **Gonda, M. A., S. A. Aaronson, N. Ellmore, V. H. Zeve, and K. Nagashima.** 1976. Ultrastructural studies of surface features of human normal and tumor cells in tissue culture by scanning and transmission electron microscopy. J. Natl. Cancer Inst. **56:**245–263.
28. **Gorelick, R. J., S. M. Nigida, J. W. Bess, Jr., L. E. Henderson, L. O. Arthur, and A. Rein.** 1990. Noninfectious human immunodeficiency virus type 1 mutants deficient in genomic RNA. J. Virol. **64:**3207–3211.
29. **Gould, S. J., A. M. Booth, and J. E. Hildreth.** 2003. The Trojan exosome hypothesis. Proc. Natl. Acad. Sci. USA **100:**10592–10597.
30. **Hasty, A. H., M. R. Plummer, K. H. Weisgraber, M. F. Linton, S. Fazio, and L. L. Swift.** 2005. The recycling of apolipoprotein E in macrophages: influence of HDL and apolipoprotein A-I. J. Lipid Res. **46:**1433–1439.
31. **Heijnen, H. F., A. E. Schiel, R. Fijnheer, H. J. Geuze, and J. J. Sixma.** 1999. Activated platelets release two types of membrane vesicles: microvesicles by surface shedding and exosomes derived from exocytosis of multivesicular bodies and alpha-granules. Blood **94:**3791–3799.
32. **Hwang, I., X. Shen, and J. Sprent.** 2003. Direct stimulation of naive T cells by membrane vesicles from antigen-presenting cells: distinct roles for CD54 and B7 molecules. Proc. Natl. Acad. Sci. USA **100:**6670–6675.
33. **Ioannou, Y. A.** 2005. Guilty until proven innocent: the case of NPC1 and cholesterol. Trends Biochem. Sci. **30:**498–505.
34. **Jeffery, C. J.** 2003. Moonlighting proteins: old proteins learning new tricks. Trends Genet. **19:**415–417.
35. **Lahiri, D. K.** 2004. Apolipoprotein E as a target for developing new therapeutics for Alzheimer's disease based on studies from protein, RNA, and regulatory region of the gene. J. Mol. Neurosci. **23:**225–233.
36. **Lawn, S. D., T. L. Pisell, C. S. Hirsch, M. Wu, S. T. Butera, and Z. Toossi.** 2001. Anatomically compartmentalized human immunodeficiency virus replication in HLA-DR+ cells and CD14+ macrophages at the site of pleural tuberculosis coinfection. J. Infect. Dis. **184:**1127–1133.
37. **Lawn, S. D., B. D. Roberts, G. E. Griffin, T. M. Folks, and S. T. Butera.** 2000. Cellular compartments of human immunodeficiency virus type 1 replication in vivo: determination by presence of virion-associated host proteins and impact of opportunistic infection. J. Virol. **74:**139–145.
38. **Lewit-Bentley, A., S. Rety, J. Sopkova-de Oliveira Santos, and V. Gerke.** 2000. S100-annexin complexes: some insights from structural studies. Cell Biol. Int. **24:**799–802.
39. **Louder, M. K., A. Sambor, E. Chertova, T. Hunte, S. Barrett, F. Ojong, E. Sanders-Buell, S. Zolla-Pazner, F. E. McCutchan, J. D. Roser, D. Gabuzda, J. D. Lifson, and J. R. Mascola.** 2005. HIV-1 envelope pseudotyped viral vectors and infectious molecular clones expressing the same envelope glycoprotein have a similar neutralization phenotype, but culture in peripheral blood mononuclear cells is associated with decreased neutralization sensitivity. Virology **339:**226–238.
40. **Mahley, R. W.** 1988. Apolipoprotein E: cholesterol transport protein with expanding role in cell biology. Science **240:**622–630.
41. **Mahley, R. W., and S. C. Rall, Jr.** 2000. Apolipoprotein E: far more than a lipid transport protein. Annu. Rev. Genomics Hum. Genet. **1:**507–537.
42. **Marsh, M., and M. Thali.** 2003. HIV's great escape. Nat. Med. **9:**1262–1263.
43. **Martin, F., D. M. Roth, D. A. Jans, C. W. Pouton, L. J. Partridge, P. N. Monk, and G. W. Moseley.** 2005. Tetraspanins in viral infections: a fundamental role in viral biology? J. Virol. **79:**10839–10851.
44. **Morita, E., and W. I. Sundquist.** 2004. Retrovirus budding. Annu. Rev. Cell Dev. Biol. **20:**395–425.
45. **Nguyen, D. G., A. Booth, S. J. Gould, and J. E. Hildreth.** 2003. Evidence that HIV budding in primary macrophages occurs through the exosome release pathway. J. Biol. Chem. **278:**52347–52354.
46. **Nydegger, S., M. Foti, A. Derdowski, P. Spearman, and M. Thali.** 2003. HIV-1 egress is gated through late endosomal membranes. Traffic **4:**902–910.
47. **Nydegger, S., S. Khurana, D. N. Krementsov, M. Foti, and M. Thali.** 2006. Mapping of tetraspanin-enriched microdomains that can function as gateways for HIV-1. J. Cell Biol. **173:**795–807.
48. **Orenstein, J. M., M. S. Meltzer, T. Phipps, and H. E. Gendelman.** 1988. Cytoplasmic assembly and accumulation of human immunodeficiency virus types 1 and 2 in recombinant human colony-stimulating factor-1-treated human monocytes: an ultrastructural study. J. Virol. **62:**2578–2586.
49. **Ott, D. E.** 2002. Potential roles of cellular proteins in HIV-1. Rev. Med. Virol. **12:**359–374.
50. **Ott, D. E., L. V. Coren, T. D. Gagliardi, and K. Nagashima.** 2005. Heterologous late-domain sequences have various abilities to promote budding of human immunodeficiency virus type 1. J. Virol. **79:**9038–9045.
51. **Ott, D. E., L. V. Coren, D. G. Johnson, B. P. Kane, I. Sowder, R. C. Sowder II, Y. D. Kim, R. J. Fisher, X. Z. Zhou, K. P. Lu, and L. E. Henderson.** 2000.

Actin-binding cellular proteins inside human immunodeficiency virus type 1. Virology **266:**42–51.
52. **Ott, D. E., L. V. Coren, B. P. Kane, L. K. Busch, D. J. Johnson, I. Sowder, R. C., E. N. Chertova, L. O. Arthur, and L. E. Henderson.** 1996. Cytoskeletal proteins inside human immunodeficiency virus type 1 virions. J. Virol. **70:** 7734–7743.
53. **Parker, S. D., J. S. Wall, and E. Hunter.** 2001. Analysis of Mason-Pfizer monkey virus Gag particles by scanning transmission electron microscopy. J. Virol. **75:**9543–9548.
54. **Pelchen-Matthews, A., B. Kramer, and M. Marsh.** 2003. Infectious HIV-1 assembles in late endosomes in primary macrophages. J. Cell Biol. **162:**443–455.
55. **Pelchen-Matthews, A., G. Raposo, and M. Marsh.** 2004. Endosomes, exosomes and Trojan viruses. Trends Microbiol. **12:**310–316.
56. **Peng, J., J. E. Elias, C. C. Thoreen, L. J. Licklider, and S. P. Gygi.** 2003. Evaluation of multidimensional chromatography coupled with tandem mass spectrometry (LC/LC-MS/MS) for large-scale protein analysis: the yeast proteome. J. Proteome Res. **2:**43–50.
57. **Pisell, T. L., I. F. Hoffman, C. S. Jere, S. B. Ballard, M. E. Molyneux, S. T. Butera, and S. D. Lawn.** 2002. Immune activation and induction of HIV-1 replication within CD14 macrophages during acute Plasmodium falciparum malaria coinfection. AIDS **16:**1503–1509.
58. **Powell, E. E., and P. A. Kroon.** 1994. Low density lipoprotein receptor and 3-hydroxy-3-methylglutaryl coenzyme A reductase gene expression in human mononuclear leukocytes is regulated coordinately and parallels gene expression in human liver. J. Clin. Investig. **93:**2168–2174.
59. **Raposo, G., M. Moore, D. Innes, R. Leijendekker, A. Leigh-Brown, P. Benaroch, and H. Geuze.** 2002. Human macrophages accumulate HIV-1 particles in MHC II compartments. Traffic **3:**718–729.
60. **Rappsilber, J., Y. Ishihama, and M. Mann.** 2003. Stop and go extraction tips for matrix-assisted laser desorption/ionization, nanoelectrospray, and LC/MS sample pretreatment in proteomics. Anal. Chem. **75:**663–670.
61. **Ryzhova, E. V., R. M. Vos, A. V. Albright, A. V. Harrist, T. Harvey, and F. Gonzalez-Scarano.** 2006. Annexin 2: a novel human immunodeficiency virus type 1 Gag binding protein involved in replication in monocyte-derived macrophages. J. Virol. **80:**2694–2704.
62. **Saito, H., P. Dhanasekaran, F. Baldwin, K. H. Weisgraber, S. Lund-Katz, and M. C. Phillips.** 2001. Lipid binding-induced conformational change in human apolipoprotein E. Evidence for two lipid-bound states on spherical particles. J. Biol. Chem. **276:**40949–40954.
63. **Sherer, N. M., M. J. Lehmann, L. F. Jimenez-Soto, A. Ingmundson, S. M. Horner, G. Cicchetti, P. G. Allen, M. Pypaert, J. M. Cunningham, and W. Mothes.** 2003. Visualization of retroviral replication in living cells reveals budding into multivesicular bodies. Traffic **4:**785–801.
64. **Strack, B., A. Calistri, S. Craig, E. Popova, and H. G. Gottlinger.** 2003. AIP1/ALIX is a binding partner for HIV-1 p6 and EIAV p9 functioning in virus budding. Cell **114:**689–699.
65. **Tabb, D. L., L. L. Smith, L. A. Breci, V. H. Wysocki, D. Lin, and J. R. Yates III.** 2003. Statistical characterization of ion trap tandem mass spectra from doubly charged tryptic peptides. Anal. Chem. **75:**1155–1163.
66. **Tardif, M. R., and M. J. Tremblay.** 2003. Presence of host ICAM-1 in human immunodeficiency virus type 1 virions increases productive infection of $CD4^+$ T lymphocytes by favoring cytosolic delivery of viral material. J. Virol. **77:**12299–12309.
67. **Tedla, N., E. N. Glaros, U. T. Brunk, W. Jessup, and B. Garner.** 2004. Heterogeneous expression of apolipoprotein-E by human macrophages. Immunology **113:**338–347.
68. **Thery, C., M. Boussac, P. Veron, P. Ricciardi-Castagnoli, G. Raposo, J. Garin, and S. Amigorena.** 2001. Proteomic analysis of dendritic cell-derived exosomes: a secreted subcellular compartment distinct from apoptotic vesicles. J. Immunol. **166:**7309–7318.
69. **Thery, C., L. Zitvogel, and S. Amigorena.** 2002. Exosomes: composition, biogenesis and function. Nat. Rev. Immunol. **2:**569–579.
70. **Tomasselli, A. G., J. O. Hui, L. Adams, J. Chosay, D. Lowery, B. Greenberg, A. Yem, M. R. Deibel, H. Zurcher-Neely, and R. L. Heinrikson.** 1991. Actin, troponin C, Alzheimer amyloid precursor protein and pro-interleukin 1b as substrates of the protease from human immunodeficiency virus. J. Biol. Chem. **266:**14548–14553.
71. **Tremblay, M. J., J. F. Fortin, and R. Cantin.** 1998. The acquisition of host-encoded proteins by nascent HIV-1. Immunol. Today **19:**346–351.
72. **Trubey, C. M., E. Chertova, L. V. Coren, J. M. Hilburn, C. V. Hixson, K. Nagashima, J. D. Lifson, and D. E. Ott.** 2003. Quantitation of HLA class II protein incorporated into human immunodeficiency type 1 virions purified by anti-CD45 immunoaffinity depletion of microvesicles. J. Virol. **77:**12699–12709.
73. **Veenstra, T. D., T. P. Conrads, and H. J. Issaq.** 2004. What to do with "one-hit wonders"? Electrophoresis **25:**1278–1279.
74. **Vogt, V. M., and M. N. Simon.** 1999. Mass determination of Rous sarcoma virus virions by scanning transmission electron microscopy. J. Virol. **73:**7050–7055.
75. **von Schwedler, U. K., M. Stuchell, B. Muller, D. M. Ward, H. Y. Chung, E. Morita, H. E. Wang, T. Davis, G. P. He, D. M. Cimbora, A. Scott, H. G. Krausslich, J. Kaplan, S. G. Morham, and W. I. Sundquist.** 2003. The protein network of HIV budding. Cell **114:**701–713.
76. **Wubbolts, R., R. S. Leckie, P. T. Veenhuizen, G. Schwarzmann, W. Mobius, J. Hoernschemeyer, J. W. Slot, H. J. Geuze, and W. Stoorvogel.** 2003. Proteomic and biochemical analyses of human B cell-derived exosomes. Potential implications for their function and multivesicular body formation. J. Biol. Chem. **278:**10963–10972.
77. **Yu, L. R., T. P. Conrads, T. Uo, Y. Kinoshita, R. S. Morrison, D. A. Lucas, K. C. Chan, J. Blonder, H. J. Issaq, and T. D. Veenstra.** 2004. Global analysis of the cortical neuron proteome. Mol. Cell Proteomics **3:**896–907.
78. **Zhu, P., E. Chertova, J. Bess, Jr., J. D. Lifson, L. O. Arthur, J. Liu, K. A. Taylor, and K. H. Roux.** 2003. Electron tomography analysis of envelope glycoprotein trimers on HIV and simian immunodeficiency virus virions. Proc. Natl. Acad. Sci. USA **100:**15812–15817.
79. **Zhu, X., and I. A. Papayannopoulos.** 2003. Improvement in the detection of low concentration protein digests on a MALDI TOF/TOF workstation by reducing alpha-cyano-4-hydroxycinnamic acid adduct ions. J. Biomol. Tech. **14:**298–307.